

Electrochemical Sensor Based on Biochar Decorated with Gold Clusters for Sensitive Determination of Acetaminophen

Qi Yu^{1,2}, Jin Zou^{1,2}, Qihui Xiong¹, Guanwei Peng², Feng Gao², Guorong Fan^{1,*},
Shangxing Chen¹, Limin Lu^{2,*}

¹ College of Forestry, Jiangxi Agricultural University, National Forestry and Grassland Bureau Woody Spice (East China) Engineering Technology Research Center, Nanchang, 330045, China

² Key Laboratory of Chemical Utilization of Plant Resources of Nanchang, College of Chemistry and Materials, Jiangxi Agricultural University, Nanchang 330045, PR China

*E-mail: fgr008@126.com (G. Fan), lulimin816@hotmail.com (L. Lu).

Received: 10 December 2021 / Accepted: 29 January 2022 / Published: 4 March 2022

Herein, a new sensing platform based on Au nanoclusters and biochar (AuNCs/BC) composite was successfully fabricated for electrochemical detection of acetaminophen (AC). BC was firstly obtained through pyrolysis of biomass of *Soulangena* sepals at 800 °C, which was served as carrier for in-situ growth of AuNCs. The designed AuNCs/BC sensor combines the AC adsorption of BC and the good conductivity and electrocatalytic activity of AuNCs, displaying good electrocatalytic activity toward AC oxidation. Differential pulse voltammetry shows that the current signal enhances linearly with AC concentration ranging from 3.0 nM to 50 µM. The limit of detection is 1.0 nM. Besides, the system shows good stability and selectivity, and has been applied to determine AC in serum samples.

Keywords: Electrochemical sensor; Biochar; Gold clusters; Acetaminophen detection

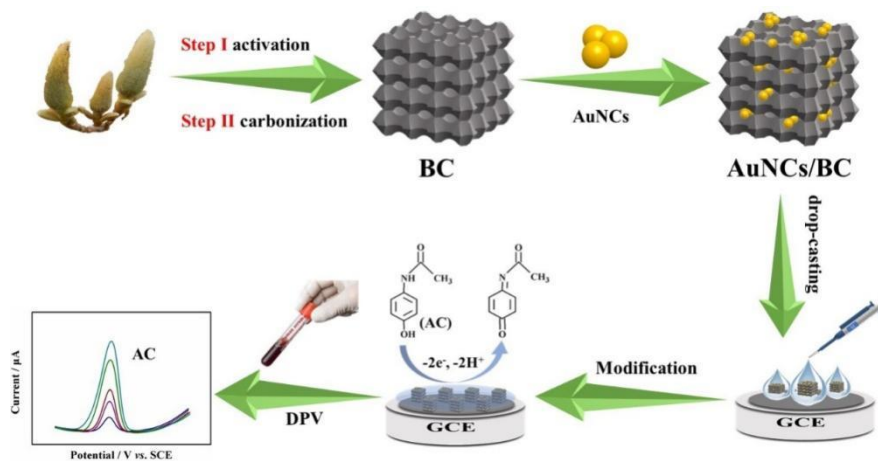
1. INTRODUCTION

As one of non-steroidal anti-inflammatory drugs, acetaminophen (AC) can be efficiently used to alleviate fever [1,2]. When suffering headaches, lumbago and skelalgia, AC can also be utilized as an analgesic to relieve the pain. However, overdose or chronic usage of AC would cause diarrhea, vomiting, abdominal pain, sweating, nausea, seizures and confusion [3-6]. Hence, developing sensitive, accurate and simple methods for detecting AC is extremely urgent. Up to now, many techniques have applied for AC detection, such as chemiluminescence [7], gas chromatography [8], spectrophotometry [9] and high-performance liquid chromatography [10-13], etc. Nevertheless, some deficiencies, like complex pretreatment, long operation time and high cost, make these methods imperfect. In contrast,

electrochemical analysis techniques have received widespread attention due to simple sample preparation, quick response, low cost and high sensitivity [14, 15].

In the electrochemical sensing analysis system, sensing material is always known as the main influencing factor on the performance such as sensitivity and responsiveness [16, 17]. In recent years, biochar (BC), a carbonaceous material obtained by controlled pyrolysis of biomass in a low amount of oxygen has received great attention promising electrode material [18-20]. The surface activity and surface structure of biochar could be effectively modulated with KOH [21], which endow it high conductivity, large specific surface areas, and high catalytic activity [22]. Hence, the material was utilized for the construction of various electrochemical sensors to detect different organic and inorganic species [23-25]. On the other hand, metal nanoparticles (NPs) own unique physicochemical properties that endow them fit for sensing applications [26]. As a typical example, gold NPs (AuNPs) are widely accepted as an sensing material to strengthen the analytical performance, owing to the advantages such as excellent catalytic activity, high specific surface area and stability [27, 28]. These advantages of BC and AuNPs motivate us to combine BC with AuNPs to construct an effective sensing platform for AC detection.

In this study, AuNCs and BC composite was used to fabricate an electrochemical sensor for AC detection. BC was employed as enrichment component for AC and served as supporter for in-situ growth of AuNCs. The obtained AuNCs could greatly improve the conductivity of BC as well as enhance the electrocatalytic activity. The synergistic effect of AuNCs and BC facilitates the electrochemical response to AC. Consequently, the prepared sensor exhibits high performance in AC sensing.



Scheme 1. Synthetic route for the preparation of AuNCs/BC sensing platform.

2. EXPERIMENTAL

2.1 Materials and reagents

Acetaminophen (AC), KOH, $\text{HAuCl}_4 \cdot \text{H}_2\text{O}$, $\text{K}_4\text{Fe}(\text{CN})_6$, $\text{K}_3\text{Fe}(\text{CN})_6$, $\text{FeCl}_3 \cdot 6\text{H}_2\text{O}$, H_3PO_4 , NaH_2PO_4 , Na_2HPO_4 , chitosan, sodium borohydride and hydrochloric acid were received from Aladdin (Shanghai, China). Soulangeana sepals were obtained from the botanical garden of Jiangxi Agricultural

University (Nanchang, China). Deionized water was utilized in all the experiment. Phosphate buffer solution (PBS, 0.1 M) with different pH was acquired by using 0.1 M Na_2HPO_4 and 0.1 M NaH_2PO_4 . All the reagents were analytically pure.

2.2 Apparatuses

Scanning electron microscope (SEM, S-4300, Germany) was applied to characterize the composites. All electrochemical experiments were conducted by using the traditional three-electrode system by a CHI760E workstation (Shanghai, China), which includes glassy carbon working electrode (GCE), saturated calomel reference electrode and platinum wire counter electrode.

2.3 Preparation of BC

The *Soulangeana* sepals were firstly washed with deionized water to removal of impurities, which were dried at 70 °C for 12 h and used grinded into the powder. Subsequently, the powder (3 g) and KOH (6 g) were dispersed in deionized water (50 mL), and got mixed thoroughly. After stirring at 25 °C for 24 h, the mixture was centrifuged and dried to obtain the activated solid sample. The dry solids were carbonized with an argon gas atmosphere for 2 h at 800 °C. The products were washed with 0.5 M HCl and deionized water till the waste solution became neutral, and finally dried in vacuum.

2.4 Preparation of AuNCs/BC composite

BC (0.50 g) was dispersed in distilled water (100 mL). 1.619 mL of HAuCl_4 (30 mM) was added to this solution under stirring. 20 min later, 10.0 mL NaBH_4 (50 mM) was dropwise added into the mixture. The whole experiment was carried out in an ice bath. After stirring for 5 h, the AuNCs/BC composite was acquired through centrifugation.

2.5 Preparation of modified electrodes

5 mg AuNCs/BC was dispersed in 1 mL chitosan acetic acid solution ($0.7 \text{ mg}\cdot\text{mL}^{-1}$) to obtained the composite dispersion. Before modification, bare GCEs were polished with $0.05 \mu\text{m}$ Al_2O_3 slurries, followed by sonicating with deionized water. 5.0 μL dispersion solution (5 mg/mL) was then casted onto the GCE surface, followed by drying under the infrared lamp, aimed at obtaining AuNCs/BC/GCE. Under the same procedure, BC/GCE was prepared.

2.6 Electrochemical measurements

Various modified electrodes were characterized by EIS with the frequency range of 0.01 ~ 100 000 Hz and the amplitude of 5 mV. Cyclic voltammetry (CV) was recorded at the potential from 0.1 to

0.8 V in 0.1 M PBS. Differential pulse voltammetry (DPV) was accustomed to detect AC in different concentration. The parameters of DPV analyses were listed in details as follows: Amplitude: 0.05 V; Pulse period: 0.5 s; Pulse width: 0.05 s; potential range: $-0.1 \sim 1.0$ V.

2.7 Preparation of biological samples

Human serum samples were obtained in Jiangxi Agricultural University Hospital, which collected on healthy volunteers. Large particle impurities in these samples were removed by centrifugation. The human serum sample was diluted with 0.1 M PBS (pH 7.0) by 100-fold, which was stored in the refrigerator (4°C) before use.

3. RESULT AND DISCUSSION

3.1 Material characterization

SEM was used to examine the microstructures and morphological features of BC and AuNCs/BC samples. As shown in Figure 1A, BC has a honeycomb-like porous structure with abundant nanoscale and micron-scale pores. From Figure 1B, it can be found that large number of particles grew on BC surface. These observations indicate that the AuNCs are relatively uniformly reduced on the BC skeleton by the reduction effect of sodium borohydride.

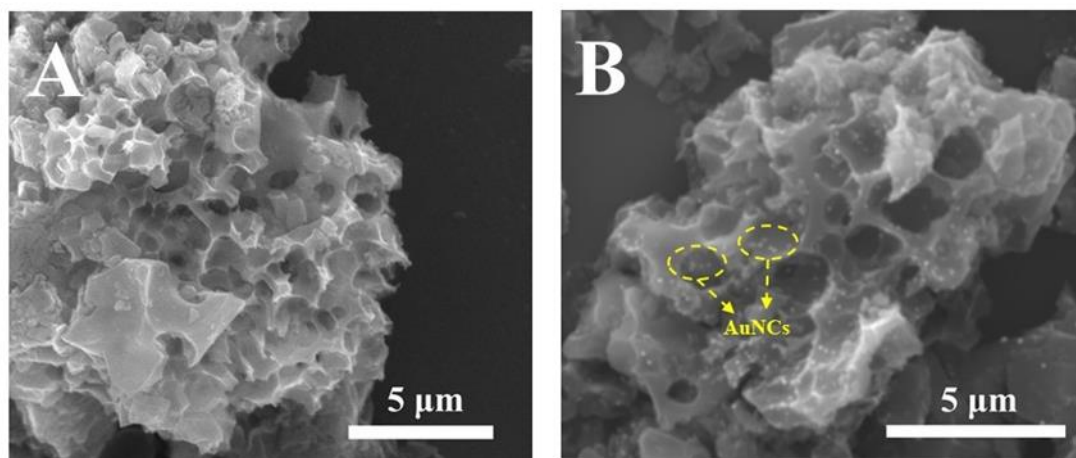


Figure 1. SEM images of BC (A) and AuNCs/BC (B).

The electron transfer characteristics of the modified electrodes were investigated by electrochemical impedance spectroscopy (EIS). The Nyquist plots of bare GCE (a), BC/GCE (b) and AuNCs/BC/GCE (c) were displayed in Figure 2. Impedance spectra usually contain a low frequency straight line and a high frequency semicircle, which correspond to the diffusion limit process and charge

transfer resistance (R_{ct}), respectively. The corresponding equivalent circuit (inset of Figure 2) is composed of the charge transfer resistance (R_{ct}), the Warburg impedance (Z_W), active electrolyte resistance (R_s) and constant phase element (CPE), which is deployed to fit the impedance data. As shown, BC/GCE (b) displays a lower R_{ct} (244 Ω) compared with bare GCE (a) (376 Ω), indicating superior conductivity of BC. Furthermore, the introduction of AuNCs on BC (c) causes a much lower R_{ct} of 62 Ω , which is owing to the truth that Au facilitates the electronic transmission on the electrode, and improves the conductivity of BC.

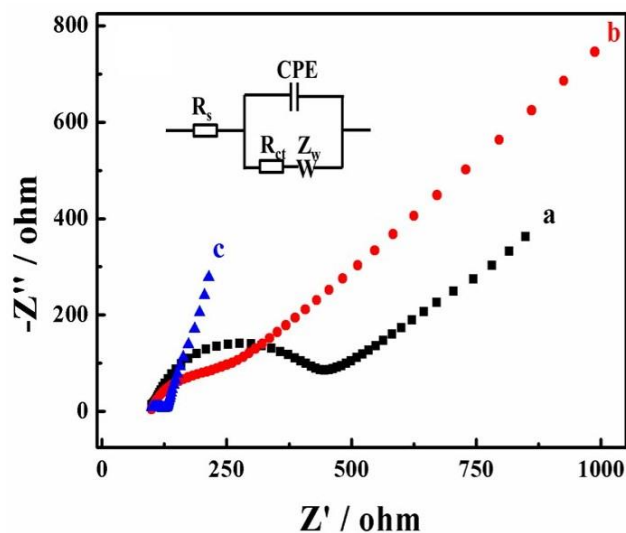


Figure 2. Nyquist plot of bare GCE (a), BC/GCE (b) and AuNCs/BC/GCE (c) in 0.1 M KCl containing 5.0 mM $[\text{Fe}(\text{CN})_6]^{3-/4-}$.

On the basis of Anson equation [29]: $Q(t) = 2nFAcD^{1/2}t^{1/2}/\pi^{1/2} + Q_{dl} + Q_{ads}$, the active surface areas of bare GCE (a), BC/GCE (b), and AuNCs/BC/GCE (c) (Figure 3A) were measured. Where, t and D are respectively the scanning time and the standard diffusion coefficient. The A is the area of effective surface and n is electrons transferred number. Based on the slope of $Q-t^{1/2}$ curves in Figure 3B, the A of AuNCs/BC/GCE (c') was measured to be 0.475 cm^2 , which is larger than bare GCE (a') (0.071 cm^2) and BC/GCE (b') (0.208 cm^2). Obviously, AuNCs/BC/GCE has the large effective surface area, which provides more catalytic sites for AC oxidation, consequently improving the current response.

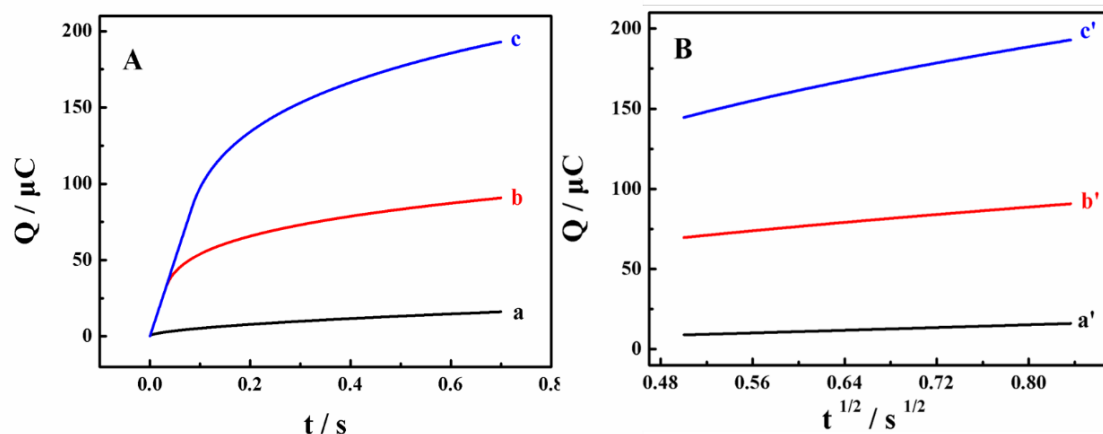


Figure 3. (A) Plot of Q - t curves of bare GCE (a), BC/GCE (b) and AuNCs/BC/GCE (c) in 0.1 mM $K_3[Fe(CN)_6]$ containing 1.0 M KCl; (B) Plot of Q - $t^{1/2}$ curves of bare GCE (a'), BC/GCE (b') and AuNCs/BC/GCE (c').

3.2 Electrochemical behavior for the oxidation of AC at various modified electrodes

Electrochemical behaviors of AC (20.0 μ M) in PBS (pH= 7.0, 0.1 M) at the modified GCEs were discussed by DPV (Figure 4). As observed, no oxidation peak is found on bare GCE (a), which is due to slowness of electronic transmission kinetics on bare GCE (a). In contrast, there is an obvious oxidation peak at BC/GCE (b), ascribing to its high conductivity and surface area. Moreover, AuNCs/BC/GCE (c) exhibits much higher anodic peak current, which is about 3 times greater than the anodic peak current of BC/GCE. These phenomena confirm that AuNCs/BC/GCE possess good electrocatalytic activity toward the oxidation of AC.

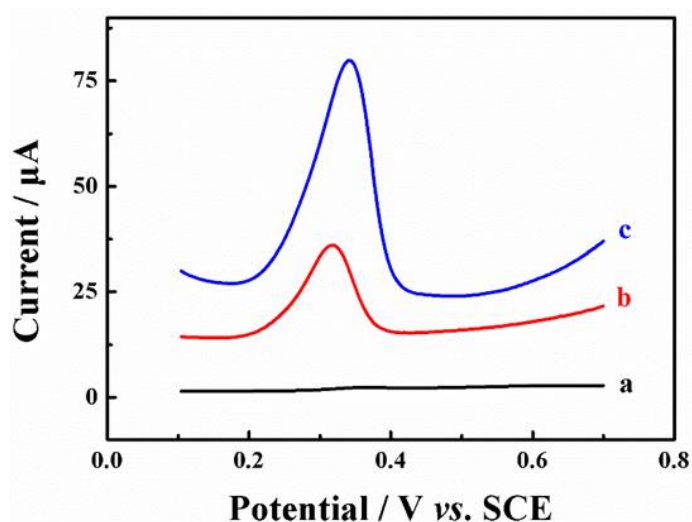


Figure 4. (B) DPVs behaviors of AC (20.0 μ M) in 0.1 M PBS (pH 7.0) on bare GCE (a), BC/GCE (b) and AuNCs/BC/GCE (c) with pulse width is 0.05 s and the amplitude is 50 mV. Accumulation time: 210 s.

3.3 Optimization of experimental parameters

The effect of solution pH value (4.0-9.0) on the oxidation peak potential and current of AC (20.0 μM) was investigated by CV. As observed from Figure 5A, the oxidation peak potential slowly moves negatively as the pH increase. The maximum current is found at pH 7.0. Therefore, PBS with pH of 7.0 is chosen the electrolyte.

Furthermore, peak potential displays a good linear relationship with pH (Figure 5B). The regression equation is $E_{pa} = 0.769 - 0.053 \text{ pH}$ ($R^2 = 0.990$), and its slope is $-0.053 \text{ mV}\cdot\text{pH}^{-1}$, which is approximately Nernstian value of $-0.059 \text{ mV}\cdot\text{pH}^{-1}$. This result indicates that in the electrode reaction, electron transfer is accompanied by an equal amount of proton [30].

The effect of enrichment time on the current of 20.0 μM AC at AuNCs/BC/GCE was studied by DPV method. As observed (Figure 5C), the peak current increases rapidly as the accumulation time increases from 0 to 210 s, and then levels off for further prolonging accumulation time. This result is owned to the saturated adsorption of AC at the modified electrode. So, the optimum accumulation time is chosen as 210 s.

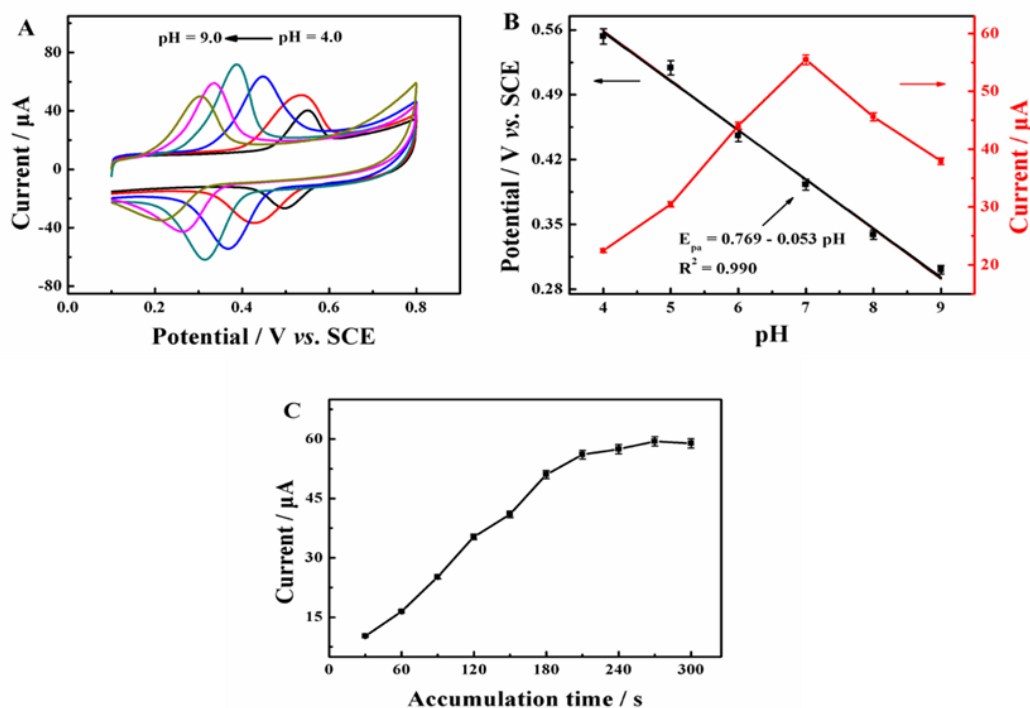


Figure 5. (A) DPV of 20.0 μM AC determined by AuNCs/BC/GCE in PBS with pH from 4.0 to 9.0; Accumulation time: 210 s. Scan rate: 100 mV s^{-1} ; (B) Effect of pH value on the anodic peak potentials and anodic peak currents. (C) Influence of accumulation time on the peak current of AC (20.0 μM) at AuNCs/BC/GCE in 0.1 M PBS (pH 7.0).

3.4 Electrochemical reaction kinetic of AC at AuNCs/BC/GCE

To study the electrochemical reaction kinetics, the effect of scan rate on the electrochemical behavior of AC (20.0 μM) at AuNCs/BC/GCE was studied using CV. As observed from Figure 6A,

there exist an increment of the oxidation peak currents (I_{pa}) and reduction peak currents (I_{pc}) with the increasing scan rate. The peak currents and the scan rates show good linearity (Figure 6B). The regression equations are $I_{pa} = 0.517 v + 2.842$ ($R^2 = 0.991$) and $I_{pc} = -0.500 v + 1.830$ ($R^2 = 0.991$). The results reveal that the electrocatalytic oxidation toward AC is an adsorption controlled process on AuNCs/BC/GCE.

Moreover, it can be seen that the redox peaks have hardly changed with the variation of scan rate in Figure 6A. The redox reaction of AC on AuNCs/BC/GCE can be considered to be reversible. E_{pa} and E_{pc} present linear relationships with napierian logarithm of the scan rate ($\ln v$) from 40 to 200 mV s^{-1} . The equations are $E_{pa} = 0.231 + 0.038 \ln v$ ($R^2 = 0.992$) and $E_{pc} = 0.461 - 0.036 \ln v$ ($R^2 = 0.992$) (Figure 6 C). On the basis of Laviron equation [31]:

$$E_{pa} = E^0 + (RT/\alpha nF) \ln(RT k^0/\alpha nF) + (RT/\alpha nF) \ln v;$$

$$E_{pc} = E^0 + \{RT/(1-\alpha)nF\} \ln\{RT k^0/(1-\alpha)nF\} - \{RT/(1-\alpha)nF\} \ln v.$$

Where, n denotes the number of transferred electrons. The values of n and α are estimated to be about 2 and 0.5. Therefore, the oxidation reaction of AC at AuNCs/BC/GCE is a two-electron and two-proton process.

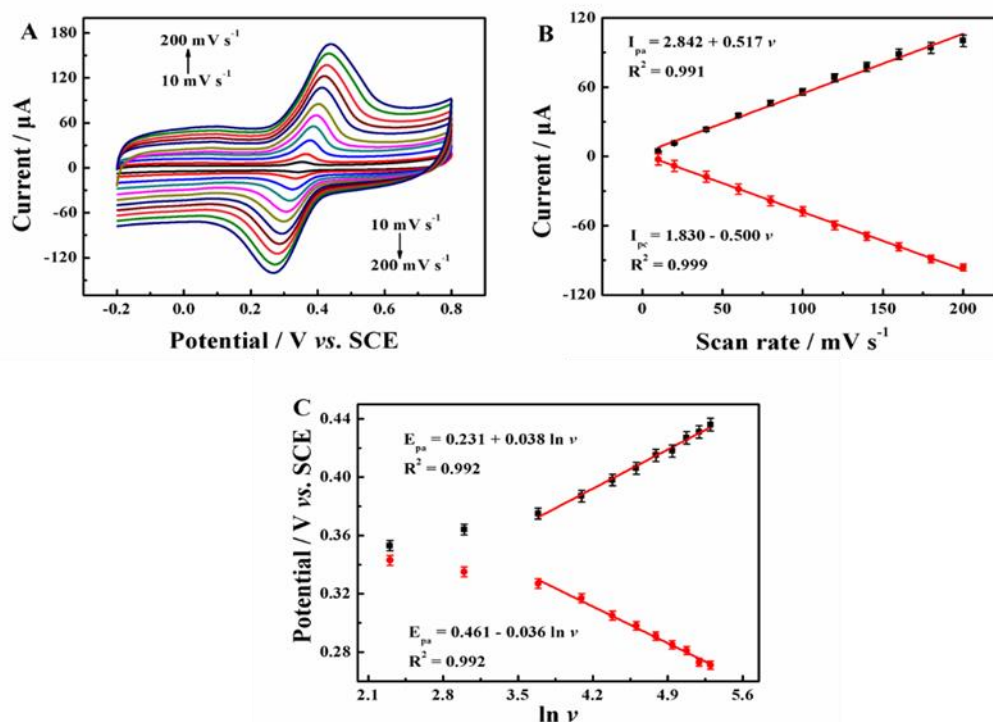


Figure 6. (A) CVs of 20 μM AC at AuNCs/BC/GCE in 0.1 M PBS (pH 7.0) with different scan rates: 10, 20, 40, 60, 80, 100, 120, 140, 160, 180 and 200 mV s^{-1} ; Accumulation time: 210 s; (B) Linear relationship between the peak current (I_{pa} and I_{pc}) and the scan rates. (C) The relationship between the redox peak potentials and $\ln v$.

3.5 Electrochemical detection of AC at AuNCs/BC/GCE

The electrochemical performance of the AuNCs/BC/GCE for AC detection was studied by DPV. Figure 7A reveals the DPV curves of AuNCs/BC/GCE with diverse concentrations of AC. As shown,

with increasing AC concentration, the peak currents gradually enhance. Besides, the current response exhibits a fine linear relationship with concentrations in the extent from 3.0 nM to 50.0 μM , which can be showed as $I (\mu\text{A}) = 0.85 + 11.96 c^{1/2} (\mu\text{M})$ ($R^2 = 0.998$) (Figure 7B). The low detection limit of AC is 1.0 nM ($S/N = 3$), which is smaller than that of the reported voltammetric approaches (shown in table 1), indicating that AuNCs/BC/GCE is an ideal sensor for AC detection.

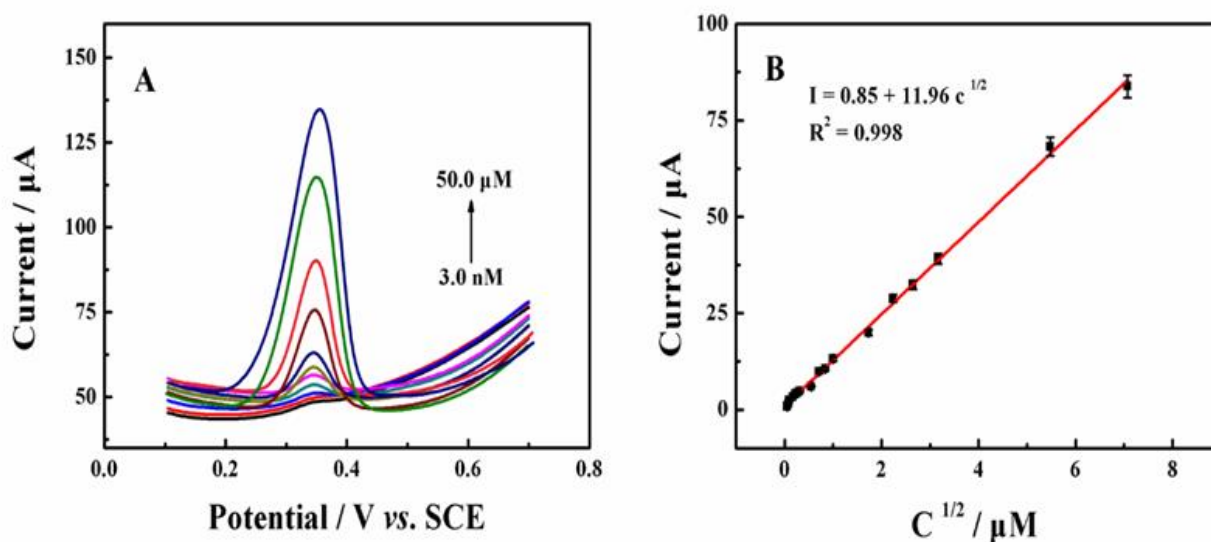


Figure 7. (A) DPV responses at AuNCs/BC/GCE in 0.1 M PBS (pH 7.0) containing different concentrations of AC (0.003, 0.007, 0.01, 0.05, 0.1, 0.5, 1.0, 5.0, 10.0, 30.0 and 50.0 μM); (B) The linear relationship between the square root of concentration and the peak current.

Table 1. Comparison of the analytical performances at AuNCs/BC/GCE with different electrochemical sensors for the determination of AC.

Modified electrodes	Linear range (μM)	LOD (nM)	Reference
BC/ Co_3O_4 / FeCo_2O_4 /GCE	0.1 - 220	28.86	[32]
ZnO- MoO_3 -C/GCE	2.5 - 2000	1140	[33]
Fc-S-Au/C NC ^a /graphene/GCE	0.5 - 275	100	[34]
PB-MWCNTs-COOH ^b /ZIF-67/GCE	0.01 - 70.0	3.3	[35]
AuNPs@TCnA ^c /GN ^d /GCE	0.5 - 120	100	[36]
AuNCs/BC/GCE	0.003 - 50	1.0	This work

^a Au/C NC: Gold nanoparticles/carbon dots nanocomposite;

^b MWCNTs: The negatively charged carboxylated multi-walled carbon nanotubes;

^c TCnA: Thiolated calix[n]arene (TCnA, n = 4, 6, 8);

^d GN: Graphene nanosheets.

3.6 Reproducibility, selectivity, repeatability and stability

To evaluate the reproducibility of the AuNCs/BC/GCE, five parallel modified electrodes were utilized to detect 20.0 μM AC in 0.1 M PBS (pH 7.0). The relative standard deviation (RSD) is 2.12% (Figure 8A), which indicates the excellent reproducibility. Furthermore, the repeatability of the sensor was investigated by fifteen times consecutive DPV measurements on one AuNCs/BC/GCE in PBS containing 20.0 μM AC. The RSD is 1.71% (Figure 8C), indicating the outstanding repeatability of AuNCs/BC/GCE.

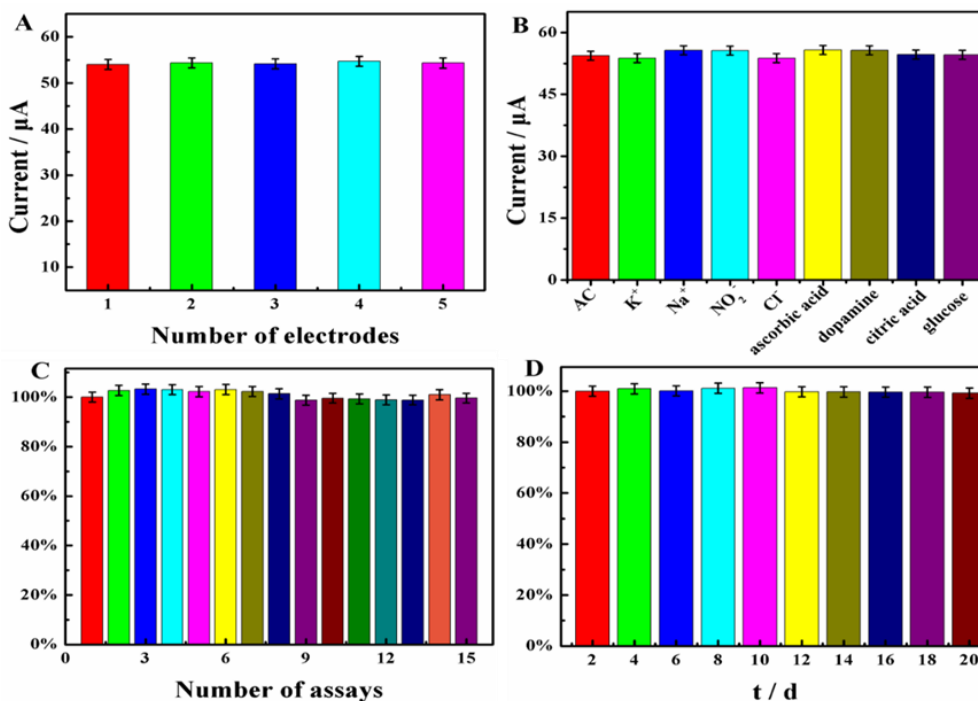


Figure 8. Reproducibility (A), selectivity (B), repeatability (C) and stability (D) of the AuNCs/BC/GCE.

In order to estimate the selectivity of the AuNCs/BC/GCE, we added some potential interfering substances into the PBS containing 20.0 μM AC and investigated the change of DPV current response. As can be seen in Figure 8B, 100-fold concentration of K⁺, Na⁺, Cl⁻, NO₂⁻ and 10-fold concentration of glucose, dopamine, citric acid, ascorbic acid show no effect toward the oxidation current of AC, indicating good selectivity.

The long-term stability of AuNCs/BC/GCE was also tested over twenty days, and the current response towards 20.0 μM AC was measured every 2 day. As observed (Figure 8D), the change of the peak current is less than 5.0% compared with the initial response current. The result manifests the AuNCs/BC/GCE has good long-term stability.

3.7 Determination of AC in human serum samples analysis

To examine the usability of the sensor, the AuNCs/BC/GCE was utilized to detect AC in human serum samples by the standard addition method. Before measuring, the samples were prepared as represented in section 2.7. The recoveries are estimated by the addition of known concentrations of AC (0, 1.0, 2.0, 5.0, 10.0 μM) into sample solutions. As observed from Table 2, the recoveries range from 97.00% to 102.00% and the RSDs are from 1.53% to 2.02%, which indicate the applied potentiality of the sensor in human serum samples.

Table 2. Recovery measurements of AC in human serum samples using the AuNCs/BC/GCE (n=5).

Human serum samples	Added (μM)	Detected (μM)	RSD (%)	Recovery (%)
1	0	-	-	-
2	1.00	1.02	1.75	102.00
3	2.00	1.96	2.02	98.00
4	5.00	4.85	1.93	97.00
5	10.00	10.03	1.53	100.30

4. CONCLUSIONS

In this work, AuNCs/BC composite was used as sensing material for the fabrication of a new electrochemical method for AC detection. The AuNCs/BC composite has several advantages, such as high electrocatalytic performance, good conductivity, high AC enrichment capacity and large specific surface area. Thanks to these unique features, the designed electrochemical sensor displays excellent analytical properties in term of good reproducibility, repeatability, wide linear range and low detection limit. The proposed sensor can detect AC in human serum samples.

ACKNOWLEDGEMENT

We are grateful to the National Natural Science Foundation of China (51862014 and 22064010), the Key R & D Program of Jiangxi Province (20192ACB60011), the Natural Science Foundation of Jiangxi Province (20202ACBL213009 and 20212BAB203019), and Special Research on Camphor Tree of Jiangxi Province Department of Forestry (2020CXZX07) for their financial support of this work.

References

1. J. Pandey, A. Ali and A.K. Gupta, *Asian J Pharm Clin Res.*, 10 (2017) 62.
2. W. Badri, K. Miladi, Q.A. Nazari, H. Gerges, H. Fessi and A. Elaissari, *Int. J. Pharm.*, 515 (2016) 757.
3. Y. Teng, L. Fan, Y. Dai, M. Zhong, X. Lu and X. Kan, *Biosens. Bioelectron.*, 71 (2015) 137.
4. F.C. Vicentini, P.A. Pereira, B.C. Janegitz, S. Machado and O. Filho, *Sens. Actuator B-Chem.*, 227 (2016) 610.
5. W. Zhang, L. Zong, S. Liu, S. Pei, Y. Zhang, X. Ding, B. Jiang and Y. Zhang, *Biosens. Bioelectron.*, 131 (2019) 200.
6. K. Annadurai, V. Sudha, G. Murugadoss and R. Thangamuthu, *J. Alloy. Compd.*, 852 (2021) 156911.
7. D. Easwaramoorthy, Y. Yu and H. Huang, *Anal. Chim. Acta.*, 439 (2001) 95.
8. D.J. Speed, S.J. Dickson, E.R. Cairns, and N.D. Kim, *J. Anal. Toxicol.*, 25 (2001) 198.
9. Sirajuddin, A.R. Khaskheli, A. Shah, M.I. Bhangar, A. Niaz and S. Mahesar, *Spectroc. Acta Pt. A.*, 68 (2007) 747.
10. C. Nebot, S.W. Gibb and K.G. G, *Anal. Chim. Acta.*, 598 (2007) 87.
11. M.E El-Kommos, N.A Mohamed and A.F. Hakiem, *J. Liq. Chromatogr. Relat. Technol.*, 35 (2012) 2188.
12. Y.M Issa, M. Hassouna, A. Zayed, *J. Liq. Chromatogr. Relat. Technol.*, 35 (2012) 2148.
13. A.P. Dewani, S.M. Dabhade, R.L. Bakal, C.K. Gadewar, A.V. Chandewar and S. Patra, *Arab. J. Chem.*, 8 (2015) 591.
14. X. Qiu, L. Lu, J. Leng, Y. Yu, W.M. Wang, M. Jiang, L. Bai, *Food Chem.* 190 (2016) 889.
15. W. Zhong, F. Gao, J. Zou, S. Liu, M.F. Li, Y. Gao, Y. Yu, X. Wang, L. Lu, *Food Chem.* 360 (2021) 130006.
16. Y. Wang, Y. Xiong, J. Qu, J. Qu and S. Li, *Sens. Actuators B.*, 223 (2016) 501.
17. N. Yang, G.M. Swain and X. Jiang, *Electroanalysis.*, 28 (2016) 27.
18. M. Vithanage, I. Herath, S. Joseph, J. Bundschuh, N. Bolan, Y. Ok and M.B. Kirkham, *Carbon.*, 113 (2017) 219.
19. A.G. Pandolfo and A.F. Hollenkamp, *J. Power Sources.*, 157 (2006) 11.
20. H. Yuan, Y. Hou, I.M. Abu-Reesh, J. Chen and Z. He, *Mater. Horizons.*, 3 (2016) 365.
21. H.H. Lima, M. Llop, R. Maniezzo, M. Moises, V. Janeiro and P. Arroyo, *J. Hazard. Mater.*, 416 (2021) 126.
22. A.E. Bailón-García, A.F. Pérez-Cadenas, F.J. Maldonado-Hódar and F. Carrasco-Marín, *Electrochim. Acta.*, 229 (2017) 219.
23. S. Xie, M. Li, Y. Liao, Q. Qin, S. Sun, and Y. Tan, *Chemosphere.*, 273 (2021) 128.
24. L. Cao, Z. Kang, Q. Ding, X. Zhang, H. Lin, M. Lin, and D. Yang, *Carbon.*, 723 (2020) 138008.
25. X. Chen, K. Lu, D. Lin, Y. Li, S. Yin, Z. Zhang, and M. Tang, *Electroanalysis.*, 32 (2020) 473.
26. F. Bettazzi, C. Ingrosso, P.S. Sfragano, V. Pifferi, L. Falciola, M. Curri and I. Palchetti, *Food Chem.*, 344 (2021) 128.
27. K. Turcheniuk, R. Boukherroub and S. Szunerits, *J. Mater. Chem. B.*, 3, (2015) 4301.
28. Y. Xiang, H. Liu, J. Yang, Z. Shi, Y. Tan, J. Jin, R. Wang, S. Zhang and J. Wang, *Electrochim. Acta.*, 261 (2018) 464.
29. F.C. Anson, *Anal. Chem.*, 36 (1964) 932.
30. D. Nematollahi, H. Shayani-Jam, M. Alimoradi and S. Niroomand, *Electrochim. Acta.*, 54 (2009) 7407.
31. E. Laviron, *Interfacial Electrochem.*, 52 (1974) 355.
32. Z. Lu, J. Zhong, Y. Zhang, M. Sun, P. Zou, H. Du, X. Wang, H. Rao and Y. Wang, *J. Alloy. Compd.*, 858 (2021) 157.
33. C. Liu, N. Zhang, X. Huang, Q. Wang, X. Wang and S. Wang, *Microchem J.*, 161 (2021) 105.

34. L. Yang, N. Huang, Q. Lu and Meiling. Liu, *Anal. Chim. Acta.*, 903 (2016) 69.
35. F. Gao, J. Zou, W. Zhong, X. Tu, X. Huang, Y. Yu, X. Wang, L. Lu and L. Bai, *Nanotechnology.*, 32 (2021) 085.
36. W. Liu, Q. Shi, G. Zheng, J. Zhou and M. Chen, *Anal. Chim. Acta.*, 1075 (2019)

© 2022 The Authors. Published by ESG (www.electrochemsci.org). This article is an open access article distributed under the terms and conditions of the Creative Commons Attribution license (<http://creativecommons.org/licenses/by/4.0/>).